Pulmonary Macrophage Subpopulations in the Induction and Resolution of Acute Lung Injury

Laura K. Johnston[1], Cliff R. Rims[1], Sean E. Gill[1,2], John K. McGuire[1,3], and Anne M. Manicone[1,2]

[1]Center for Lung Biology, and [2]Division of Pulmonary and Critical Care Medicine, University of Washington, Seattle, Washington; and [3]Department of Pediatrics, Children's Hospital of Seattle, Seattle, Washington

Macrophages are key orchestrators of the inflammatory and repair responses in the lung, and the diversity of their function is indicated by their polarized states and distinct subpopulations and localization in the lung. Here, we characterized the pulmonary macrophage populations in the interstitial and alveolar compartments during the induction and resolution of acute lung injury induced by *Pseudomonas aeruginosa* infection. We identified macrophage subpopulations and polarity according to FACS analysis of cell surface protein markers, combined with cell sorting for gene expression using real-time PCR. With these techniques, we validated a novel, alternatively activated (M2) marker (transferrin receptor), and we described three interstitial and alveolar macrophage subpopulations in the lung whose distribution and functional state evolved from the induction to resolution phases of lung injury. Together, these findings indicate the presence and evolution of distinct macrophage subsets in the lung that serve specific niches in regulating the inflammatory response and its resolution. Alterations in the balance and function of these subpopulations could lead to nonresolving acute lung injury.

Keywords: inflammation; infection; M1; M2; *Pseudomonas aeruginosa*; pneumonia

CLINICAL RELEVANCE

Macrophages contribute to both the induction and resolution phases of acute lung injury (ALI). This study characterizes the phenotypes of macrophage subpopulations in the lung interstitium and alveolar space during the induction and resolution of ALI. Understanding this heterogeneity of pulmonary macrophages will be important in developing strategies to modulate lung injury.

Acute lung injury (ALI) is a clinical disease marked by respiratory failure attributable to the disruption of the epithelial and endothelial barrier, flooding of the alveolar compartment with protein-rich fluid, and the recruitment of neutrophils into the alveolar space (1). Although neutrophil influx and activation within the lung are important contributors to the pathogenesis of ALI (2–11), increasing evidence indicates that macrophages also contribute to the modulation of inflammatory responses (11, 12), the resultant lung injury (13–15), and importantly, the resolution of these responses.

Based on patterns of gene expression, protein secretion, and roles in host defense, macrophages have been classified into classically activated (M1) and alternatively activated (M2) macrophages, although a continuum of macrophage polarization likely exists beyond these discrete *in vitro*–based classifications (16). The M1 phenotype is induced by proinflammatory Th1 cytokines, such as IFN-γ and LPS, and is characterized by the production of high concentrations of proinflammatory factors, including IL-1β, IL-12, TNF-α, and inducible nitric oxide synthase (iNOS). The M2 phenotype can be induced by the Th2 cytokines IL-4 and IL-13, and is characterized by the production of anti-inflammatory molecules such as IL-10. Unlike other discrete leukocyte populations, macrophages maintain their plasticity and can alter their phenotype based on the microenvironment, including cytokine milieu among other factors. For example, M1 cells can repolarize toward M2 after the phagocytosis of apoptotic neutrophils (17, 18), suggesting that reprogramming inflammatory macrophages toward an M2 phenotype may be involved in the resolution phase of ALI.

Macrophage influx into the lung occurs during the induction and resolution phases of lung inflammation, and previous studies demonstrated that the increased recruitment of macrophages to the lungs using monocyte chemotactic protein-1 was associated with attenuated lung injury (19). However, other studies, including those using macrophage depletion techniques, indicate that macrophages also contribute to the pathogenesis of lung injury (20). One explanation of these disparate effects of macrophages in ALI may relate to the heterogeneity of monocytes and macrophages, and the selective depletion or altered recruitment of proinflammatory and anti-inflammatory populations of these leukocytes. Further characterization of these subpopulations in pulmonary disease may allow for therapeutic interventions in which the recruitment of subpopulations of macrophages may be exploited to modify disease.

In our experiments, we used a murine model of pneumonia to study the macrophage subpopulations recruited or differentiated within the interstitial and alveolar spaces of the lung. We used gene expression and the cell-surface expression of M1 and M2 markers across three interstitial and alveolar pulmonary macrophage populations during the induction and resolution of ALI, and found unique, nonoverlapping expression profiles within these populations. We identified resident macrophage populations ($CD11b^{low}CD45^{high}$) with the greatest M1 phenotype during the induction of ALI, and the early presence of M2 ($CD11b^{int}CD45^{int}$) cells during the induction phase of ALI that we hypothesize could modify the initial inflammatory response. We also identified the recruitment of $CD11b^{high}CD45^{high}$ macrophages that coexpressed M1 and M2 markers during the induction of lung injury and that were later the predominant M2 cells during the resolution phase. Together, these cell populations likely fine-tune the immune system, and the failure of these transitions or the recruitment of regulatory macrophage subpopulations may contribute to the pathogenesis of nonresolving ALI.

(*Received in original form March 6, 2012 and in final form May 30, 2012*)

This work was supported by a Howard Hughes Medical Institute Physician Scientist Early Career Award, and by National Institutes of Health grants HL084385 (A.M.M.), HL098067, HL089455, and HL093022.

Correspondence and requests for reprints should be addressed to Anne M. Manicone, M.D., Center for Lung Biology, University of Washington, 815 Mercer Street, Seattle, WA 98109. E-mail: manicone@u.washington.edu

This article has an online supplement, which is accessible from this issue's table of contents at www.atsjournals.org

Am J Respir Cell Mol Biol Vol 47, Iss. 4, pp 417–426, Oct 2012

Originally Published in Press as DOI: 10.1165/rcmb.2012-0090OC on June 21, 2012
Internet address: www.atsjournals.org

MATERIALS AND METHODS

Mice

C57BL/6NTac mice, male or female, aged 8 to 12 weeks, were used for all experiments. Mice were housed in microisolator cages under specific pathogen–free conditions. All animal experiments were approved by the Institutional Animal Care and Use Committees at the University of Washington.

Exposure Models

The *Pseudomonas aeruginosa* strain PAK was grown in LB broth, as described elsewhere (21). Mice received a high-dose deposition of 1×10^7 bacteria/lung via oropharyngeal aspiration. To assess initial bacterial deposition, two mice were killed after delivery for the quantitative culture of whole-lung homogenates. The remaining mice ($n = 5$ mice/time point) were killed at 1, 2, 3, 4, and 7 days after infection. The lungs were lavaged three times with 1.0 ml PBS + 0.5 mM EDTA for the determination of cell counts and differential, total protein, and IgM concentrations. The left lung was removed and homogenized in PBS for quantitative bacterial culture. In separate experiments, nonlavaged lungs were collected for immunohistochemistry.

Quantitative RT-PCR

Total RNA from lung tissue or sorted macrophages was isolated with the RNeasy Mini kit (Qiagen, Valencia, CA) and processed as previously described (21). See the online supplement for details on analysis.

Macrophage Culture

Bone marrow cells from the femur/tibia were harvested and selected using 20% L929 medium as described elsewhere (21). After 1 week, bone marrow–derived macrophages (BMDMs) were replated, and then untreated (M0) macrophages were stimulated with *Escherichia coli* LPS O111:B4 (100 ng/ml) for 24 hours (M1), or with IL-4/IL-13 (10 ng/ml each; Invitrogen, Grand Island, NY) for 48 hours (M2). After stimulation, cells were harvested and labeled with several rat anti-murine antibodies, including CD11b, intercellular adhesion molecule (ICAM)-I, transferrin receptor, CD40, CD206 (Abcam, Cambridge, MA), and MAC2 (Cedarlane, Burlington, NC). The secondary antibody was FITC-conjugated anti-rat (Abcam). Cells were analyzed using the BD FACSCanto II Flow Cytometer (BD Biosciences, San Jose, CA), and analysis was performed using FlowJo software (Tree Star, Inc., Ashland, OR).

Flow Cytometry

Murine lungs were lavaged with PBS + 2 mM EDTA using 1.0, 0.9, and 0.9 ml serially. Cardiac perfusion was performed using 10 ml of PBS. The lungs were dissociated in C Tubes using a gentleMACS Dissociator (Miltenyi Biotec, Auburn, CA), and digested using Liberase TM (1 mg/ml; Roche, Indianapolis, IN) and DNase I (1 mg/ml; Sigma Aldrich, St. Louis, MO) for 10 minutes at 37°C. Lung digests were filtered through a 70-μm nylon cell strainer (Becton Dickinson, Franklin Lakes, NJ), and erythrocytes were removed using RBC Lysis Buffer (eBioscience, San Diego, CA). For immunostaining, bronchoalveolar lavage and lung homogenate cells were washed with 0.5% FBS and 2 mM EDTA in PBS, and counted using Easycount (Immunicon, Huntingdon Valley, PA). Cells were labeled with antibodies, as described in the online supplement.

Immunostaining

Murine lungs were fixed in 10% formalin and paraffin-embedded. Sections were deparaffinized using Histoclear (National Diagnostics, Atlanta, GA) and rehydrated through graded ethanol. Antigen retrieval was performed using Bond HIER 2 (Leica Microsystems, Buffalo Grove, IL) for 20 minutes at 100°C. Sections were incubated with rabbit anti-iNOS (Millipore, Billerica, MA) or rabbit IgG for 30 minutes at 21°C, and then with Leica Bond Polymer DAB Refine, Peroxide Block and Mixed Refine DAB detection (Leica Microsystems). Counterstaining was performed using Harris hematoxylin (Leica Microsystems).

RESULTS

Murine Pneumonia Model Time-Course Study

We used a bacterial model of pneumonia, based on a clinical isolate of *Pseudomonas aeruginosa* to produce acute lung injury. To characterize the temporal course of pulmonary inflammation and injury, mice were analyzed for leukocytic influx into the interstitium and bronchoalveolar space on Days 1, 2, 3, 4, and 7 after infection with 1×10^7 bacteria/lung (Figure 1). The characterization of lung injury was performed by assessing BAL total protein and IgM concentrations (Figures 1E and 1F) as well as histology for the degree of inflammation and alveolar wall thickness (not shown).

We found that peak neutrophil influx into the alveolar space occurred on Day 2, macrophage influx into the alveolar space occurred by Day 2 and peaked on Day 4, and lymphocyte influx started on Day 2 concurrent with macrophage influx, and peaked and remained elevated on Days 3 to 7 (Figures 1A–1D). Using protein and IgM concentration in BAL fluid as a marker of lung injury, we found that protein concentrations in the alveolar space increased acutely by Day 1, and remained elevated until Day 3 (Figures 1E and 1F). Between Days 3 and 4, total protein concentrations trended downward, marking the resolution phase of lung injury. Based on these experiments, we further characterized macrophage phenotypes from Days 0, 1, 4, and 7 to capture both the induction and resolution stages of lung injury.

M1 and M2 Gene Expression Markers in Whole Lung and Alveolar Cells

We hypothesized that M1 markers (TNF-α, IL-6, and i-NOS) would be rapidly induced or up-regulated in infected lungs, and that M2 markers (found in inflammatory zone 1 [FIZZ-1], arginase 1 [ARG-1], and IL-10) would be induced or up-regulated during the resolution phase of lung injury and inflammation. We examined the gene expression of these M1 and M2 markers in RNA isolated from alveolar cells and lavaged whole-lung RNA. As expected, M1 markers peaked early on Day 1, during the induction phase of inflammation and injury (Figure 2A). Unlike the M1 markers, the M2 genes appeared to have a bimodal distribution (Figure 2B), and peaked during the induction and resolution phases. IL-10 demonstrated two peaks, especially apparent in the interstitial compartment. FIZZ-1 demonstrated two peaks in the alveolar compartment, but one peak during the resolution phase in the interstitial cells. We also determined the expression of these markers according to nonleukocyte and leukocyte populations in the lung, using a magnetic selection of $CD45^+$ cells. We found that all the iNOS expression and a majority of the IL-6, IL-10, TNF-α, and ARG-1 expression came from leukocytes (data not shown). We also determined iNOS protein expression in lung tissue, using immunohistochemistry (Figure 2C). We found that iNOS protein peaked on Day 2, and remained detectable in macrophages up to Day 7, closely following the trend of gene expression in the interstitial compartment.

Identification of M1 and M2 Markers

To determine the phenotype of macrophage populations, we chose among a panel of potential M1 and M2 markers originally identified by Becker and colleagues, who used plasma membrane proteomics from polarized murine macrophages (22). Among those markers identified by Becker and colleagues (22), ICAM-1 and CD40 were found to be present in the M1 membrane proteome, and transferrin receptor (TfR) was found to be present in the M2 membrane proteome. Other proteins were shared across polarized states, such as CD11b and galectin-3 (MAC2). We used

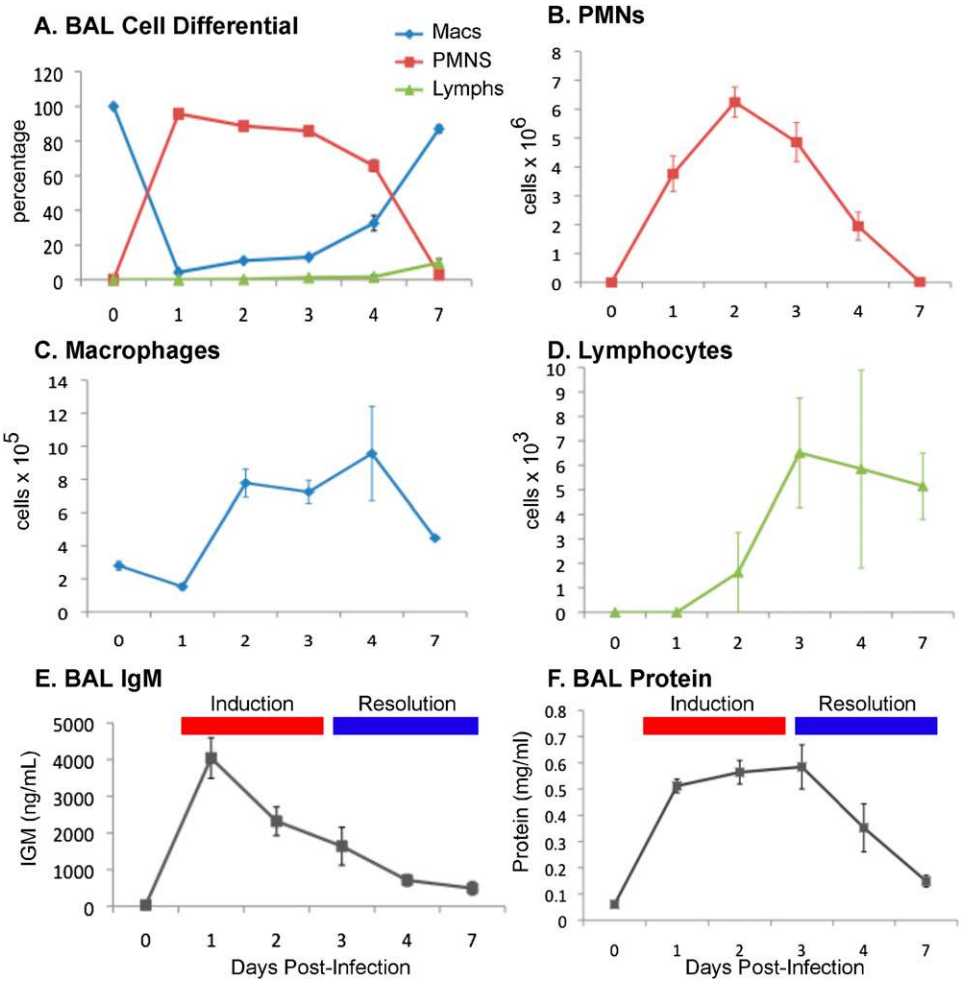

Figure 1. Pulmonary inflammatory response in *Pseudomonas aeruginosa* pneumonia. Mice were infected with *P. aeruginosa* (1×10^7 organisms) via oropharyngeal aspiration ($n = 4$ mice/time point). Bronchoalveolar lavage (BAL) fluid was collected, and samples were processed for cell counts and differentials on Days 1, 2, 3, 4, and 7. (*A*) BAL fluid cell differential was performed on 100 cells per sample, and as percentages of cells, neutrophils represented the majority of the cells from Days 1–4. The BAL fluid cell counts are reported for (*B*) neutrophils, (*C*) macrophages, and (*D*) lymphocytes, and both macrophages and lymphocytes increased in cell numbers from Days 2 to 4. (*E*) BAL fluid IgM concentration and (*F*) total protein, markers of vascular leakage, peaked early. Combined with the resolution of neutrophil counts, these parameters defined the induction and resolution phases of lung injury. PMNs, polymorphonuclear leukocytes.

flow cytometry of BMDMs at rest (M0) or stimulated with LPS (M1) or IL-4/IL-13 (M2) to assess the protein expression of these macrophage markers. We found that M1 cells demonstrated the greatest expression of both ICAM-1 and CD40 compared with the other macrophage populations (Figure 3, *middle*). We also found that TfR was most highly expressed by M2 cells, outperforming an established M2 marker, the mannose receptor (Figure 3, *right*). Because ICAM-1 and TfR showed the greatest changes associated with M1 and M2 polarization, respectively, these markers were chosen to evaluate polarized states, using macrophages isolated from murine lung tissue.

Identification of Interstitial Macrophage Populations Using FACS and Cell Sorting

Our gene expression data already suggest that the alveolar macrophage population polarizes to an inflammatory macrophage upon exposure to bacteria, and also suggest divergent roles of the interstitial macrophage population. To explore the macrophage populations in the interstitium and alveolar space, we collected and homogenized lungs from uninfected and infected mice after performing cardiac perfusion to remove intravascular leukocytes, and bronchoalveolar lavage to remove alveolar leukocytes. To identify macrophage subpopulations, we selected cells with high side scatter/forward scatter to exclude monocytes, gated on $CD45^+$ cells (leukocytes), and excluded granulocyte differentiation antigen 1 $(GR1)^{high}$ cells (neutrophils) (Figure 4A). We identified three distinct macrophage populations using both CD11b and CD45 expression (Figure 4B), and found that this combination of markers gave us the clearest separation of populations for analysis when compared with other markers such as F4/80 and GR1. We sorted and performed cytospins on these interstitial populations at each time point, and confirmed that they were macrophages in appearance (large, rounded nuclei with abundant cytoplasm), and representative images from dissociated lung tissue are shown (Figure 4C). In addition to CD11b and CD45, we analyzed cells for the expression of other antigens, including CD11c, major histocompatibility complex class II (MHCII), F4/80, GR1, ICAM-1, and TfR (Figure 5 and Figure E1 in the online supplement). To identify changes in the expression of M1 and M2 markers, ICAM-1, and TfR, we calculated the mean fluorescence intensity (MFI) for TfR (MFI^{TfR}) and ICAM-1 ($MFI^{ICAM\text{-}1}$) and their respective isotype controls (MFI^{ISO}). ΔMFI was calculated for each sample (MFI^{TfR} or $MFI^{ICAM\text{-}1} - MFI^{ISO}$), and the results are expressed as mean ΔMFI ± SEM (Figure 6).

In the naive murine lung (Day 0), $CD11b^{low}CD45^{high}$ cells represented the most abundant interstitial macrophage population (63.1% ± 2.5%). This population (Group I) most closely resembled alveolar macrophages in terms of size and antigen profile. Notably, these cells expressed CD11c (previously reported as a marker of resident alveolar macrophages) (Figure 5, Group I). Although these cells represented the majority of the interstitial macrophage population on Day 0, they decreased to 23.0%, 20.4%, and 20.8% on Days 1, 4, and 7, respectively, after infection, while other recruited macrophages ($CD11b^{high}$ $CD45^{high}$ cells) became the majority. During the induction phase of lung injury (Day 1), these cells up-regulated the M1 marker,

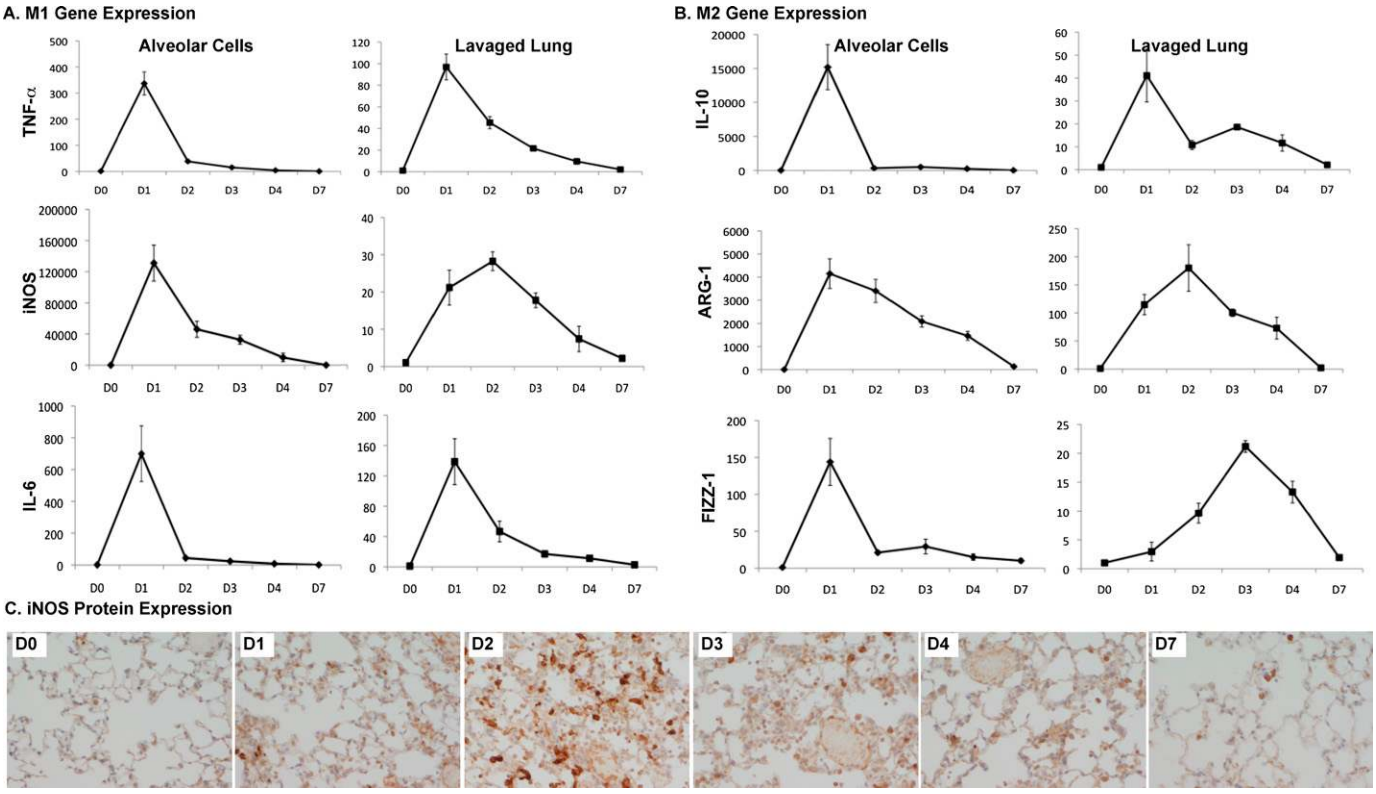

Figure 2. Expression of classically activated (M1) and alternatively activated (M2) markers in alveolar and interstitial compartments. Mice ($n = 3$–4) were infected with *P. aeruginosa* and harvested on Days (D) 1–4 and 7. Lungs were lavaged for the collection of alveolar cells, and both alveolar cells and lavaged lungs were processed for RNA. RT-PCR, using commercially available primer–probe sets for M1 (TNF-α, inducible nitric oxide synthase [iNOS], and IL-6) and M2 (IL-10, arginase 1, and found in inflammatory zone 1) markers, was performed in duplicate on all samples and normalized to the housekeeping gene, hypoxanthine-guanine phosphoribosyl transferase. Results are reported as fold increase over Day 0 (uninfected) samples. All of the M1 markers peaked early (D1–D2), whereas the M2 markers demonstrated a bimodal distribution, especially apparent in the interstitial compartment. (*C*) iNOS protein expression in lung tissue matched that of its RNA expression, with a peak on Day 2.

ICAM-1, which peaked on Day 1 and progressively deceased on Days 4 and 7, approaching its expression at rest (Day 0) (Figures 5 and 6A). These cells also increased the expression of the M2 marker, transferrin receptor, with peak expression during the resolution phase (Figures 5 and 6C). These results suggest that these resident cells rapidly polarize toward M1 during the induction of injury, and repolarize as they transition back to their resting state. A similar expression profile in ICAM-1 and TfR and similar cellular distribution were seen in the alveolar compartment, with $CD11b^{low}CD45^{high}$ cells comprising all the cells on

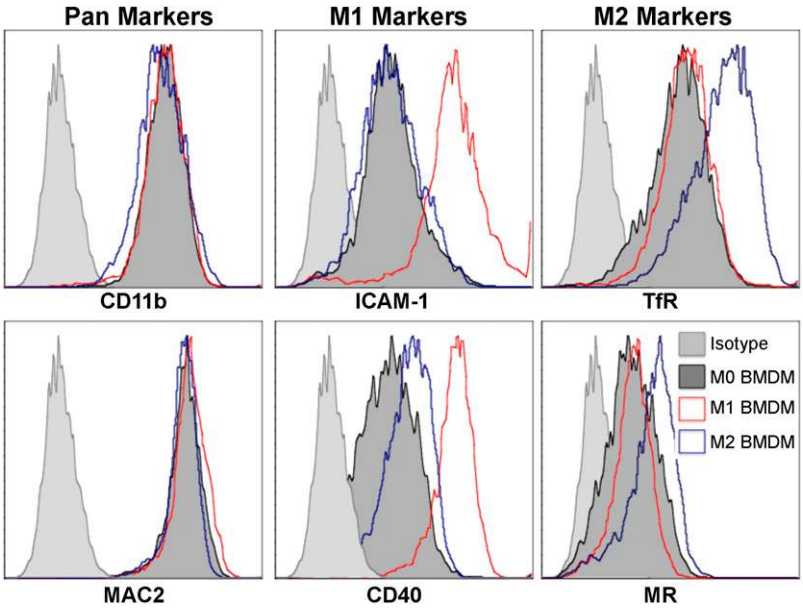

Figure 3. Intracellular adhesion molecule 1 (ICAM-1) and transferrin receptor as markers of polarized macrophages. Bone marrow–derived macrophages (BMDM) were either untreated (M0; *dark gray*), stimulated with LPS for 24 hours (M1; *red*), or stimulated with IL-4/IL-13 for 48 hours (M2; *blue*). Cells were harvested and labeled with CD11b and MAC2 (pan-markers; *left column*); ICAM-1 and CD40 (M1 markers; *middle column*); and transferrin (TfR) and mannose receptor (MR) (M2 markers; *right column*). All pan, M1, and M2 markers were expressed by all groups, but only ICAM-1 and transferrin receptor increased selectively in M1 and M2 polarized cells, respectively. Transferrin receptor, as a marker of M2 cells, was more robust than that of mannose receptor. Isotype control samples are shown (*light gray*).

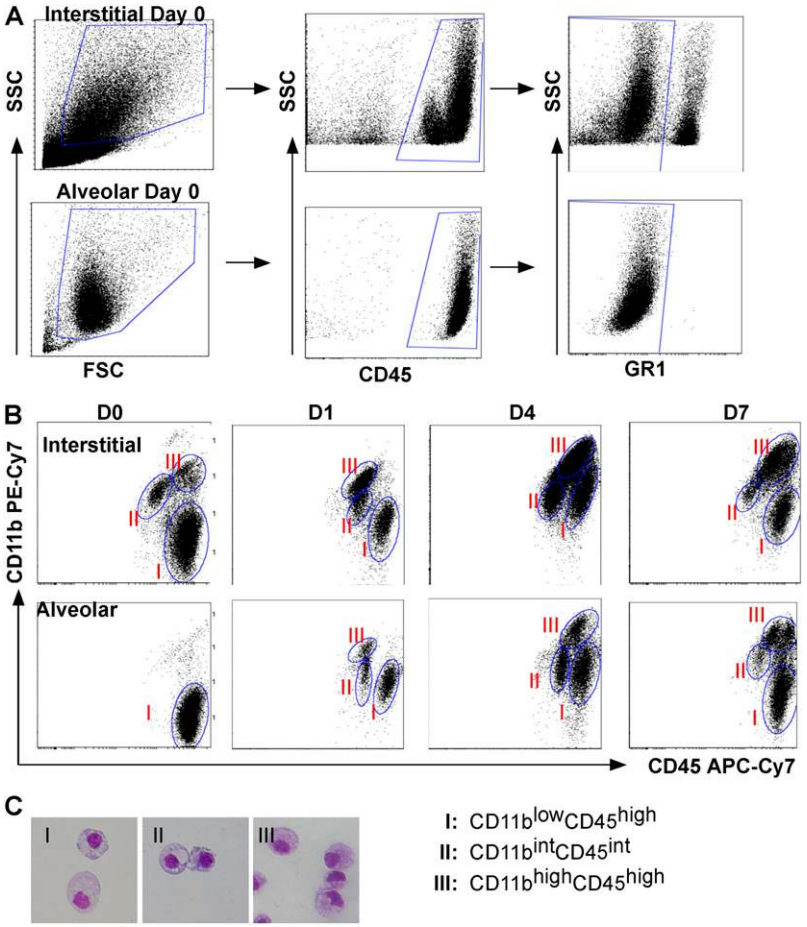

Figure 4. Identification of pulmonary macrophage subpopulations. (*A*) Subpopulation identification in interstitial (*top row*) and alveolar (*bottom row*) compartments on Day 0 was based on the following gating strategy: cells were selected according to their larger size (forward scatter [FSC]) and granularity (side scatter [SSC]) (*left*), on their CD45 expression to select leukocytes (*middle*), and on their granulocyte differentiation antigen 1 (GR-1)^{high} exclusion to remove neutrophils (*right*). (*B*) Macrophages were grouped into three populations based on CD11b and CD45 staining intensity. Shown are representative dot plots from Days 0, 1, 4, and 7 after infection with *P. aeruginosa*, identifying Group I as CD11b^{low}CD45^{high}, Group II as CD11b^{int}CD45^{int}, and Group III as CD11b^{high}CD45^{high}. (*C*) Representative cytospins of cells were sorted from Groups I–III, fixed, and stained with Diff-Quik. Cells demonstrated the appearance of macrophages, and Group III was comprised of cells with more of a kidney-shaped nucleus. APC-Cy7, allophycocyanin cyanine dye.

Day 0, and approximately 28–43% during Days 1, 4, and 7 (Figure E1 and Figures 6B and 6D). The generation of chimeras using green fluorescent protein (GFP) mice (in which a majority of resident macrophages remain GFP-negative, and recruited cells remain GFP-positive) confirmed that these cell populations (CD11b^{low}CD45^{high} from both alveolar and interstitial compartments) remained from the resident population during the experiment time course (Figure E2).

The second macrophage population identified in the interstitium on Day 0 involved CD11b^{int}CD45^{int} cells (Group II), comprising 14.4% ± 0.6% of the macrophages. These cells expressed ICAM-1 on Day 0, with a slight increase in expression after injury (Day 1), but not to the same degree as seen in the CD11b^{low}CD45^{high} population (Figure 6E). These cells did not express TfR at baseline, but a population within this group (33.9%) expressed the M2 marker on Day 1, suggesting early activation or recruitment of an M2 cell (Figure 5, Group II; Figure 6G). CD11b^{int}CD45^{int} cells were not present in the alveolar compartment on Day 0, but were present starting on Day 1, with weak TfR expression on Day 1 (Figure E1 and Figure 6H). Furthermore, an increase in CD11c expression was associated with the resolution phases (Days 4 and 7). Using GFP chimeras to identify these as recruited or resident cells, we found that these cells on Day 0 were GFP-positive, suggesting that they more readily turn over in the lung. As such, all cells recruited to the alveolar compartment were also GFP-positive (Figure E2).

The third group of macrophages identified in the interstitium on Day 0 comprised CD11b^{high}CD45^{high} cells, representing 22.5% ± 2.0% of cells on Day 0, and the majority (71.4% and 65.1%) of cells on Days 4 and 7, respectively. During the induction of ALI, these cells did not express TfR (Figure 5). However, during resolution (Days 4 and 7), an increase in TfR, MHCII, CD11c, and ICAM-1 occurred (Figure 5, Group III; Figures 6I and 6K). In the alveolar space, these cells also demonstrated peak expression of the M2 marker, TfR, during the resolution phases of lung injury (Figure E1 and Figure 6L). Using GFP chimeras, these cells represented the majority of recruited macrophages. Similar to CD11b^{int}CD45^{int} cells, they were also GFP-positive on Day 0, suggesting that in their resting state, they more readily turn over in the lung than do CD11b^{low} CD45^{high} cells (Figure E2).

M1 and M2 Gene Expression in Macrophage Subpopulations

RNA was collected from sorted interstitial and alveolar populations on Days 0, 1, 4, and 7. We used RT-PCR for several genes to help classify the polarized states of these macrophage subsets in the interstitial (Table 1) and alveolar (Table 2) compartments, including ARG-1, IL-10, TNF-α, iNOS, IL-6, IL-12, fibronectin, CCL17, CCL22, and IL-1ra. As expected, each population demonstrated its own unique expression profile of genes. The resident interstitial macrophage population (CD11b^{low}CD45^{high}), which we had identified as M1 cells on Day 1 by ICAM-1 up-regulation, exhibited the greatest increase in the proinflammatory markers TNF-α and IL-6 on Day 1 when compared with the other two populations. As we observed with TfR expression, a small increase occurred in ARG-1 (M2 marker) expression, peaking during the resolution phase (Day 4). In contrast, the CD11b^{int}CD45^{int} group showed the greatest increase in the M2 cytokines IL-10 and CCL22 on Day 1 in both compartments,

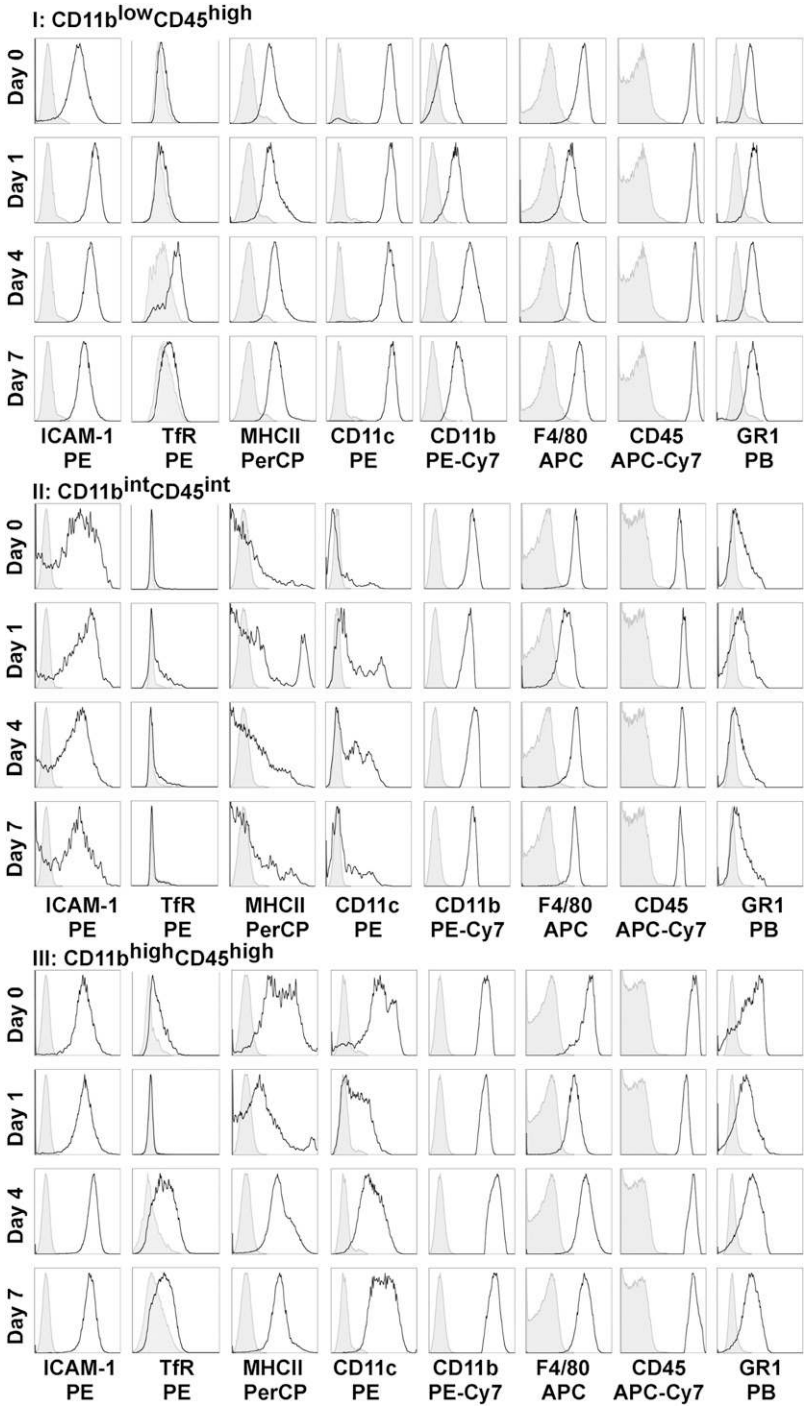

Figure 5. Cell-surface markers on pulmonary macrophage subpopulations from the interstitial compartment during the induction and resolution of acute lung injury (ALI). ICAM-1, TfR, major histocompatibility complex class II (MHCII), CD11c, CD11b, F4/80, CD45, and GR1 expression was determined according to macrophage subgroups (based on CD11b and CD45 gating) from the interstitial compartment on Days 0, 1, 4, and 7 after pneumonia. Group I ($CD11b^{low}CD45^{high}$) showed the greatest increase in ICAM-1 expression on Day 1, which decreased toward baseline during resolution (Days 4 and 7). These cells also expressed TfR during the resolution phase. Group II ($CD11b^{int}CD45^{int}$) cells expressed the M2 marker TfR on Day 1, and Group III ($CD11b^{high}CD45^{high}$) cells expressed the M2 marker TfR during the resolution phase. APC, allophycocyanin; Cy7, cyanine; PB, Pacific blue; PE, R-phycoerythrin; PerCP, peridinin chlorphyll protein complex.

suggesting that this cellular population may play distinct functional roles related to immunomodulation during the induction phase of lung injury. The $CD11b^{high}CD45^{high}$ cells were the highest expressers of iNOS, IL-12, and ARG-1. This coexpression of both M1 and M2 markers was also seen in the alveolar compartment. During resolution (Days 4 and 7), these cells were the highest expressers of fibronectin, important in wound repair responses. These cells also up-regulated the M2 marker, TfR, at these time points, suggesting that recruited $CD11b^{high}$ $CD45^{high}$ cells are the predominant reparative macrophage in the lung.

Because IL-1ra has been shown to be important in mitigating the induction of lung injury (23) and was previously reported to be abundantly expressed in exudative ($CD11b^{high}$) macrophages in the alveolar space, we sought to establish the cellular population responsible for its expression in our experiments. We found that all cell populations expressed this regulatory cytokine. However, it was most abundant in the recruited macrophages, $CD11b^{int}CD45^{int}$ and $CD11b^{high}$ $CD45^{high}$, in the alveolar space.

Nonpulmonary Macrophage Populations Also Acquire the M2 Phenotype after Infection

Concurrent with our lung isolation, we also isolated and dissociated spleen tissue from wild-type mice to analyze extrapulmonary macrophage subpopulations with the same techniques and flow cytometry markers. We identified two F4/80-positive macrophage populations in the spleen, which we identified as $CD11b^{neg}$ and

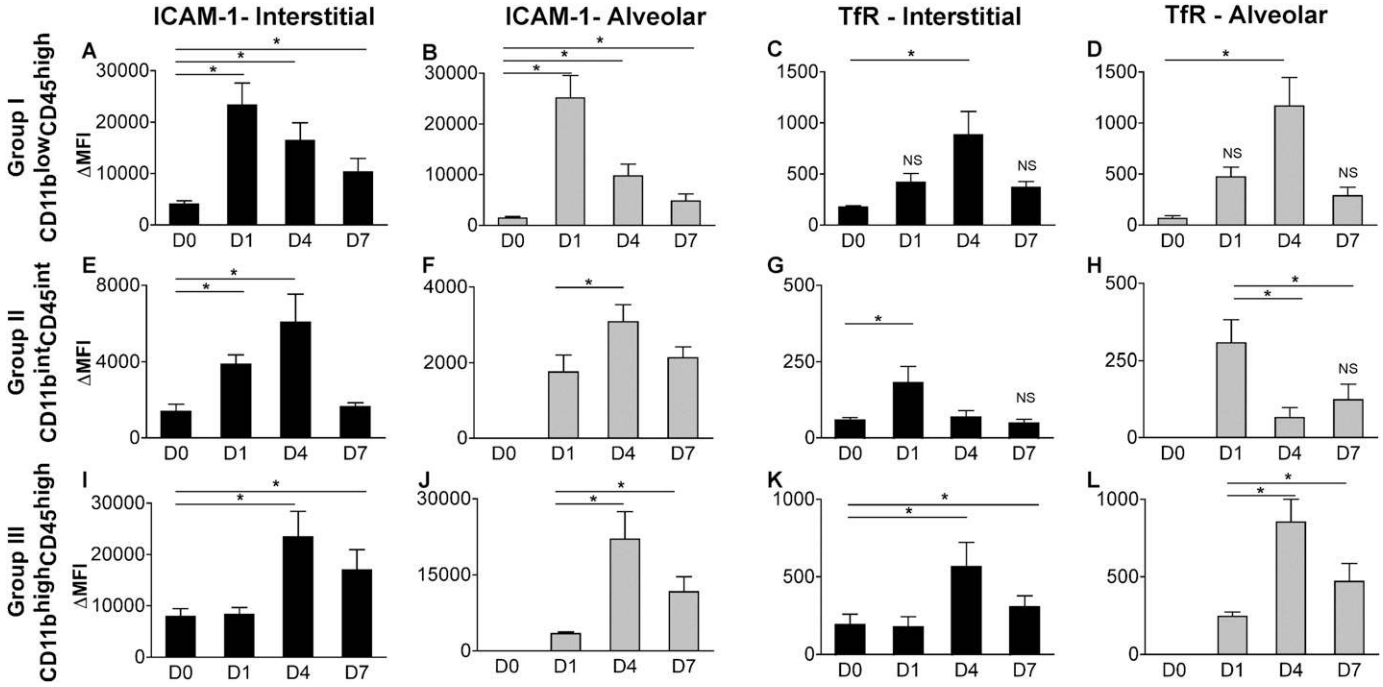

Figure 6. ICAM-1 and TfR identify polarized states of macrophage subpopulations during ALI. To identify changes in expression for ICAM-1 and TfR, we calculated the mean fluorescence intensity (MFI) for TfR, ICAM-1, and their respective isotype control samples. ΔMFI was calculated for each sample, and results are expressed as mean ΔMFI ± SEM for Group I (*top row*, *A–D*), Group II (*middle row*, *E–H*), and Group III (*bottom row*, *I–L*). Group I macrophages in both compartments (*solid bar*, interstitial; *gray bar*, alveolar) showed the greatest increase in ICAM-1 expression during the induction phase of ALI, identifying M1 polarization in these resident cells. However, ICAM-1 was also highly expressed in recruited cells (Group III) during the resolution phase. TfR expression was significantly increased during the resolution phase in Groups I and III, peaking on Day 4, and on Day 1 in Group II. $*P < 0.05$, with Day 0 or Day 1 as reference group, as already noted ($n = 6–9$ samples per time point). The significance of the raw MFI for TfR and ICAM-1 compared with their respective isotype control samples was determined using the Student *t* test. Except where indicated as nonsignificant (NS), all findings were significant at $P < 0.05$.

$CD11b^{high}$ (Figure 7). On Day 0, the predominant population was $CD11b^{neg}$ (82.9%). However, after infection, an increase in the $CD11b^{high}$ population occurred, which comprised more than 40% of the F4/80-positive macrophages on Day 4. We observed a large increase in TfR expression in the $CD11b^{high}$ population (greatest on Day 4), similar to what was observed in the $CD11b^{high}CD45^{high}$ population of cells in the lung (Figure 7). Whether these cells represent a pool of reparative cells to be recruited to the lung or changes associated with more systemic macrophage responses to injury and repair remains undetermined.

TABLE 1. RELATIVE GENE EXPRESSION OF M1 AND M2 MARKERS BY INTERSTITIAL MACROPHAGES

	$CD11b^{low}$ $CD45^{high}$	$CD11b^{int}$ $CD45^{int}$	$CD11b^{high}$ $CD45^{high}$	$CD11b^{low}$ $CD45^{high}$	$CD11b^{int}$ $CD45^{int}$	$CD11b^{high}$ $CD45^{high}$	$CD11b^{low}$ $CD45^{high}$	$CD11b^{int}$ $CD45^{int}$	$CD11b^{high}$ $CD45^{high}$
	TNF-α			IL-10†			ARG-1		
D0	1.56	0.66	1.68	0.007	0.02	0.41	0.008	0.008	0.12
D1	17.69	7.96	4.84	3.10	8.62	1.11	0.23	0.38	32.60
D4	0.81	0.49	0.61	0.21	0.37	0.70	0.58	0.51	13.01
D7	01.06	0.38	0.46	ND	0.09	0.05	0.06	0.39	1.02
	IL-6*			CCL22			iNOS		
D0	0.005	0.05	0.18	2.09	0.13	0.20	<0.001	0.001	0.001
D1	29.80	14.29	10.14	0.77	14.36	8.35	0.40	0.38	5.87
D4	0.072	0.80	0.11	0.08	0.21	0.03	0.02	0.018	0.08
D7	0.004	0.11	0.008	0.03	0.10	0.02	0.001	0.002	0.01
	IL-12*			IL-1ra			FN		
D0	0.01	0.07	0.14	0.42	1.23	0.72	21.93	7.33	18.27
D1	0.12	0.50	8.75	12.65	17.94	19.18	23.42	21.82	306.30
D4	0.05	0.05	0.14	1.39	0.98	1.36	18.96	40.67	86.88
D7	0.003	0.03	0.01	0.81	0.89	0.51	18.09	49.8	69.46

Definition of abbreviations: ARG-1, arginase 1; CCL22, C-C motif chemokine 22; D, day; FN, fibronectin; iNOS, inducible nitric oxide synthase; M1, classically activated; M2, alternatively activated.

* $\times 10^{-1}$.

† $\times 10^{-2}$.

TABLE 2. RELATIVE GENE EXPRESSION OF M1 AND M2 MARKERS BY BRONCHOALVEOLAR MACROPHAGES

	$CD11b^{low}$ $CD45^{high}$	$CD11b^{int}$ $CD45^{int}$	$CD11b^{high}$ $CD45^{high}$	$CD11b^{low}$ $CD45^{high}$	$CD11b^{int}$ $CD45^{int}$	$CD11b^{high}$ $CD45^{high}$	$CD11b^{low}$ $CD45^{high}$	$CD11b^{int}$ $CD45^{int}$	$CD11b^{high}$ $CD45^{high}$
	TNF-α			IL-10†			ARG-1		
D0	0.06			ND			0.004		
D1	0.48	5.43	4.02	0.30	3.20	0.46	0.02	4.31	29.3
D4	0.10	0.16	0.14	0.02	ND	ND	0.02	0.94	2.24
D7	0.09	0.13	0.15	ND	ND	ND	0.004	0.36	0.50
	IL-6*			CCL22			iNOS		
D0	0.002			0.06			ND		
D1	0.42	4.64	3.74	1.77	10.92	0.66	0.006	1.11	1.07
D4	0.02	1.30	0.02	0.10	8.31	0.08	ND	ND	ND
D7	ND	0.02	0.01	0.14	0.41	0.46	ND	ND	ND
	IL-12*			IL-1ra			FN		
D0	ND			1.32			6.95		
D1	0.03	17.11	16.27	4.57	25.14	25.79	10.23	35.57	20.00
D4	0.004	ND	0.01	1.40	0.92	1.56	17.17	41.63	78.08
D7	ND	ND	0.005	0.90	1.11	1.48	10.84	20.71	66.15

For definition of abbreviations, *see* Table 1.
* $\times 10^{-1}$.
† $\times 10^{-2}$.

DISCUSSION

A growing body of evidence points to the diversity of macrophages in regulating the induction of ALI and its resolution, indicating that macrophages are key regulators of both of these processes, and suggesting distinct roles for macrophage subpopulations. A move to classify subpopulations of macrophages has been based on exogenous stimuli, gene expression, and function, although much of this classification is based on *in vitro* studies. For example, M1 cells have been simplistically defined as macrophages that up-regulate proinflammatory factors such as iNOS, IL-6, IL-12, and TNF-α, whereas M2 cells down-regulate proinflammatory cytokines and express ARG-1, FIZZ-1, and transferrin receptor, among other factors. However, these polarized functions, initially described *in vitro,* likely represent a continuum, and our findings observed *in vivo* suggest that macrophages share some overlapping features.

In our experiments, we sought to phenotype the interstitial and alveolar macrophage subpopulations in a murine model of lung injury, using surface markers and gene expression, to provide a basis for future studies aimed at understanding how these distinct populations regulate the induction and resolution phases of lung injury. We chose a murine model of pneumonia induced by a clinical strain of *P. aeruginosa* as our model of ALI, and characterized the time course of leukocytic influx and protein leakage to identify the induction of ALI (Day 1) and resolution (Days 4–7) phases. We identified macrophage subpopulations using a panel of cell surface markers, and found that distinct populations were most easily identified using CD11b and CD45 staining intensity. As described by others (24), we found that CD11b intensity distinguished resident from recruited cellular populations. We also used ICAM-1 and TfR expression intensity as M1 and M2 surface markers. These markers of polarized macrophages were originally identified by Becker and colleagues, using membrane proteomics of polarized macrophages (22), and we validated these markers using FACS analysis of *in vitro* BMDMs. Using macrophages isolated from murine lung tissue, ICAM-1 was expressed by all subpopulations, especially recruited cells (as expected for an adhesion receptor involved in facilitating leukocyte endothelial transmigration). However, the magnitude of up-regulation was greatest in the resident interstitial macrophages, which also showed the largest increase in other M1 markers (TNF-α and IL-6) by gene expression. Hence, ICAM-1 is a useful marker when comparing expression intensity according to flow cytometry in this subpopulation, but we predict that other staining modalities, such as immunohistochemistry, would not constitute sensitive methods to identify M1 cells. We found that transferrin receptor expression performed well as an *in vivo* M2 marker, and was superior to mannose receptor in our *in vitro* studies. TfR was not well-expressed in resting conditions. However, it was most highly expressed on macrophages during the resolution phase of injury, and its expression corresponded to cells with reduced proinflammatory gene expression and increased markers of wound repair. This receptor has also been independently identified as an M2 marker, using IL-4/IL-13–stimulated BMDM cells (25).

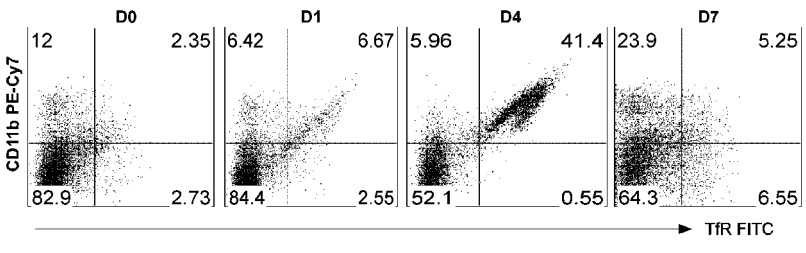

Figure 7. Systemic polarized macrophage response during the resolution of ALI. Spleens were harvested on Days 0, 1, 4, and 7 after *P. aeruginosa* pneumonia, and cells were analyzed by flow cytometry using antibodies to F4/80, CD11b, GR1, MHCII, CD45, ICAM-1, and TfR. $GR1^{high}$ cells (neutrophils), $CD45^{neg}$, and $F4/80^{neg}$ cells were excluded. The F4/80-positive macrophages were evaluated for CD11b and TfR expression, as shown. As seen in the lung, a striking increase in TfR-expressing $CD11b^{high}$ cells occurred on Day 4, with macrophage distribution returning toward baseline on Day 7.

Using these methods, we identified three distinct macrophage populations in the interstitial and alveolar space, and for the most part the alveolar and interstitial populations appeared to share similar trends in surface markers and gene expression over time. Some differences in gene expression were dependent on the compartmentalization of macrophages (interstitial versus alveolar), but overall, our evaluation of alveolar macrophage subpopulations was also informative regarding interstitial subpopulations that cannot be easily sampled in human ALI.

We identified a unique population of interstitial and alveolar macrophages on Day 1 that were high IL-10–producing and also weakly expressed the surface receptor for M2 cells. These results suggest an early recruitment or activation of a resident population of immune-modulating macrophages (M2), and this population could serve to balance the proinflammatory milieu. IL-10–producing macrophages have been described in other tissues, such as the intestine, and the intestinal milieu was proposed to require anti-inflammatory macrophage programming to limit overexuberant inflammatory responses in the gut (26). Equally important are methods of limiting inflammatory responses in the lung, and any perturbation of these cells could predispose lung tissue to worse inflammation and injury.

Our studies also identified a population of proinflammatory M1 cells within the interstitium, which were resident cells according to our GFP chimera studies. During the resolution phases of lung injury, this population ($CD11b^{low}CD45^{high}$) up-regulated the M2 marker transferrin receptor and ARG-1 gene expression, representing M1 cells in transition. A similar trend in repolarization markers was observed in these cells in the alveolar space.

Finally, we identified a $CD11b^{high}$-expressing population of cells that demonstrated the highest iNOS, IL-12, and ARG-1 gene expression on Day 1. Although this subpopulation may be comprised of smaller subgroups, the coexpression of iNOS and ARG-1 may also be representative of cells that share M1 and M2 markers. This finding has been reported by others using coimmunostaining (27), and has also been well described in myeloid-derived suppressor cells that inhibit T-cell proliferation via the coexpression of iNOS and ARG-1 and a local depletion of arginine (28). These $CD11b^{high}$ cells also expressed high amounts of IL-12, another factor by which these cells could regulate T-cell responses (29). During resolution phases, the $CD11b^{high}$ cells in the alveolar and interstitial compartments expressed the M2 surface marker TfR, and their gene expression profile demonstrated an increase in expression of genes involved in tissue repair (such as fibronectin). These results suggest that the predominant reparative or M2 macrophage in ALI is a recruited population of $CD11b^{high}$ cells. Interestingly, we observed a similar population of $CD11b^{high}$ macrophages in the spleen during the resolution phase, and these cells also exhibited a marked increase in the M2 marker TfR. These finding suggest that polarized macrophage responses are more systemic in this model of ALI; if and how these cells contribute to the resolution of ALI remain unknown. However, in mice, the spleen is a hematopoietic organ, and this may comprise one reservoir by which macrophages regulate inflammatory responses via recruitment to the lung, the production of local or systemic cytokines, or local interactions with other leukocytes, and in particular, T cells.

To our knowledge, this is the first study in which distinct macrophage subpopulations in the lung (both alveolar and interstitial) compartments were characterized by M1 and M2 cell surface markers coupled with gene expression studies, using cell sorting during the induction and resolution phases of ALI. Our findings highlight a novel surface marker to define cells with a more reparative (M2) phenotype, and provide insights into *in vivo* macrophage responses in ALI. The limitations of these experiments include their failure to capture all macrophages through gating techniques, and the possibility that additional subsets or heterogeneity may exist within our defined populations. However, this study remains a comprehensive evaluation of $CD11b^{+}$ macrophage subpopulations. These findings could form the basis of future studies in which the distinct functional roles of these cellular populations are further characterized to identify potential targets that modulate ALI.

Author disclosures are available with the text of this article at www.atsjournals.org.

Acknowledgments: The authors thank William C. Parks for helpful discussions, and Ying Wang for her assistance with murine colony maintenance.

References

1. Manicone A. Role of the pulmonary epithelium and inflammatory signals in acute lung injury. *Expert Rev Clin Immunol* 2009;5:63–75.
2. Aggarwal A, Baker CS, Evans TW, Haslam PL. G-CSF and IL-8 but not GM-CSF correlate with severity of pulmonary neutrophilia in acute respiratory distress syndrome. *Eur Respir J* 2000;15:895–901.
3. Belperio JA, Keane MP, Burdick MD, Londhe V, Xue YY, Li K, Phillips RJ, Strieter RM. Critical role for CXCR2 and CXCR2 ligands during the pathogenesis of ventilator-induced lung injury. *J Clin Invest* 2002;110:1703–1716.
4. Bhatia M, Brady M, Zagorski J, Christmas SE, Campbell F, Neoptolemos JP, Slavin J. Treatment with neutralising antibody against cytokine induced neutrophil chemoattractant (CINC) protects rats against acute pancreatitis associated lung injury. *Gut* 2000;47:838–844.
5. Kotani M, Kotani T, Ishizaka A, Fujishima S, Koh H, Tasaka S, Sawafuji M, Ikeda E, Moriyama K, Kotake Y, *et al.* Neutrophil depletion attenuates interleukin-8 production in mild-overstretch ventilated normal rabbit lung. *Crit Care Med* 2004;32:514–519.
6. Lomas-Neira JL, Chung CS, Grutkoski PS, Miller EJ, Ayala A. CXCR2 inhibition suppresses hemorrhage-induced priming for acute lung injury in mice. *J Leukoc Biol* 2004;76:58–64.
7. Mukaida N, Matsumoto T, Yokoi K, Harada A, Matsushima K. Inhibition of neutrophil-mediated acute inflammation injury by an antibody against interleukin-8 (IL-8). *Inflamm Res* 1998;47:S151–S157.
8. Sakashita A, Nishimura Y, Nishiuma T, Takenaka K, Kobayashi K, Kotani Y, Yokoyama M. Neutrophil elastase inhibitor (sivelestat) attenuates subsequent ventilator-induced lung injury in mice. *Eur J Pharmacol* 2007;571:62–71.
9. Sekido N, Mukaida N, Harada A, Nakanishi I, Watanabe Y, Matsushima K. Prevention of lung reperfusion injury in rabbits by a monoclonal antibody against interleukin-8. *Nature* 1993;365:654–657.
10. Zarbock A, Allegretti M, Ley K. Therapeutic inhibition of CXCR2 by reparixin attenuates acute lung injury in mice. *Br J Pharmacol* 2008; 155:357–364.
11. Lomas-Neira J, Chung CS, Perl M, Gregory S, Biffl W, Ayala A. Role of alveolar macrophage and migrating neutrophils in hemorrhage-induced priming for ALI subsequent to septic challenge. *Am J Physiol Lung Cell Mol Physiol* 2006;290:L51–L58.
12. Fujimoto J, Wiener-Kronish JP, Hashimoto S, Sawa T. Effects of CL2MDP-encapsulating liposomes in a murine model of *Pseudomonas aeruginosa*–induced sepsis. *J Liposome Res* 2002;12:239–257.
13. Kooguchi K, Hashimoto S, Kobayashi A, Kitamura Y, Kudoh I, Wiener-Kronish J, Sawa T. Role of alveolar macrophages in initiation and regulation of inflammation in *Pseudomonas aeruginosa* pneumonia. *Infect Immun* 1998;66:3164–3169.
14. Marriott HM, Dockrell DH. The role of the macrophage in lung disease mediated by bacteria. *Exp Lung Res* 2007;33:493–505.
15. Herold S, Steinmueller M, von Wulffen W, Cakarova L, Pinto R, Pleschka S, Mack M, Kuziel WA, Corazza N, Brunner T, *et al.* Lung epithelial apoptosis in influenza virus pneumonia: the role of macrophage-expressed TNF-related apoptosis-inducing ligand. *J Exp Med* 2008;205:3065–3077.
16. Sica A, Mantovani A. Macrophage plasticity and polarization: *in vivo veritas*. *J Clin Invest* 2012;122:787–795.
17. Taylor EL, Rossi AG, Dransfield I, Hart SP. Analysis of neutrophil apoptosis. *Methods Mol Biol* 2007;412:177–200.
18. Freire-de-Lima CG, Xiao YQ, Gardai SJ, Bratton DL, Schiemann WP, Henson PM. Apoptotic cells, through transforming growth factor–beta,

coordinately induce anti-inflammatory and suppress pro-inflammatory eicosanoid and NO synthesis in murine macrophages. *J Biol Chem* 2006;281:38376–38384.

19. Amano H, Morimoto K, Senba M, Wang H, Ishida Y, Kumatori A, Yoshimine H, Oishi K, Mukaida N, Nagatake T. Essential contribution of monocyte chemoattractant protein–1/C-C chemokine ligand–2 to resolution and repair processes in acute bacterial pneumonia. *J Immunol* 2004;172:398–409.
20. Sone Y, Serikov VB, Staub NC Sr. Intravascular macrophage depletion attenuates endotoxin lung injury in anesthetized sheep. *J Appl Physiol* 1999;87:1354–1359.
21. Manicone AM, Birkland TP, Lin M, Betsuyaku T, van Rooijen N, Lohi J, Keski-Oja J, Wang Y, Skerrett SJ, Parks WC. Epilysin (MMP-28) restrains early macrophage recruitment in *Pseudomonas aeruginosa* pneumonia. *J Immunol* 2009;182:3866–3876.
22. Becker L, Liu NC, Averill MM, Yuan W, Pamir N, Peng Y, Irwin AD, Fu X, Bornfeldt KE, Heinecke JW. Unique proteomic signatures distinguish macrophages and dendritic cells. *PLoS ONE* 2012;7:e33297.
23. Herold S, Tabar TS, Janssen H, Hoegner K, Cabanski M, Lewe-Schlosser P, Albrecht J, Driever F, Vadasz I, Seeger W, *et al.* Exudate macrophages attenuate lung injury by the release of IL-1 receptor antagonist in Gram-negative pneumonia. *Am J Respir Crit Care Med* 2011;183: 1380–1390.
24. Janssen WJ, Barthel L, Muldrow A, Oberley-Deegan RE, Kearns MT, Jakubzick C, Henson PM. Fas determines differential fates of resident and recruited macrophages during resolution of acute lung injury. *Am J Respir Crit Care Med* 2011;184:547–560.
25. Corna G, Campana L, Pignatti E, Castiglioni A, Tagliafico E, Bosurgi L, Campanella A, Brunelli S, Manfredi AA, Apostoli P, *et al.* Polarization dictates iron handling by inflammatory and alternatively activated macrophages. *Haematologica* 2010;95:1814–1822.
26. Sheikh SZ, Plevy SE. The role of the macrophage in sentinel responses in intestinal immunity. *Curr Opin Gastroenterol* 2010;26:578–582.
27. Redente EF, Higgins DM, Dwyer-Nield LD, Orme IM, Gonzalez-Juarrero M, Malkinson AM. Differential polarization of alveolar macrophages and bone marrow–derived monocytes following chemically and pathogen-induced chronic lung inflammation. *J Leukoc Biol* 2010;88:159–168.
28. Gabrilovich DI, Nagaraj S. Myeloid-derived suppressor cells as regulators of the immune system. *Nat Rev Immunol* 2009;9:162–174.
29. Metzger DW. Interleukin-12 as an adjuvant for induction of protective antibody responses. *Cytokine* 2010;52:102–107.